

Nature of well-defined conductance of amine anchored molecular junctions

Zhenyu Li and D. S. Kosov

Department of Chemistry and Biochemistry, University of Maryland, College Park, MD 20742

Amine terminated molecules show well behaved conductance in the scanning tunneling microscope break-junction experimental measurements. We performed density functional theory based electron transport calculations to explain the nature of this phenomenon. We find that amines can be adsorbed only on apex Au atom, while thiolate group can be attached equally well to undercoordinated and clean Au surfaces. Our calculations show that only one adsorption geometry is sterically and energetically possible for amine anchored junction whereas three different adsorption geometries with very distinct transport properties are almost equally probable for thiolate anchored junction. We calculated the conductance as a function of the junction stretching when the molecules are pulled by the scanning tunneling microscope tip from the Au electrode. Our calculations show that the stretching of the thiolate anchored junction during its formation is accompanied by significant electrode geometry distortion. The amine anchored junctions exhibit very different behavior – the electrode remains intact when the scanning tunneling microscope tip stretches the junction.

PACS numbers: 73.63.-b, 85.65.+h, 72.10.-d

I. INTRODUCTION

Considerable experimental and computational efforts have been devoted in recent years to molecular electronics.¹ The main goal in molecular electronics is the formation and characterization of nano-electronic device in which a molecule plays the role of a conducting element. Molecular junctions are formed by placing molecules in thin, sub-nanometer gap between metal electrodes. It is assumed that under certain conditions a single molecule bridges the gap and conducts the electricity. Although there has been a significant progress towards experimental determination of a single molecular conductance, there is growing awareness that the number of molecules which bridge the gap is not a well characterized experimental quantity. Indeed, it is difficult to prove experimentally without uncertainty that the measured value is the single molecular conductance rather than the conductance through molecular array.

In the experimental technique, which was pioneered by Tao *et al.*^{2,3,4} and then used by Venkataraman *et al.*^{5,6} for amine terminated molecules, the junctions are formed by repeatedly crashing an Au scanning tunneling microscope (STM) tip into and moving it out of Au surface in a molecular solution. The recent experiment of Venkataraman *et al.*⁵ demonstrated that amine anchored molecular junctions exhibit well-defined and experimentally stable transport properties, namely 1,4-benzenediamine (BDA) has 2-3 orders smaller variations of the conductance between different experimental measurements than 1,4-benzenedithiolate (BDT).⁵ This is a counterintuitive observation. The thiolate-Au chemical bond is considerably stronger than the amine-Au bond. Therefore, one may expect that the stronger molecule-electrode link would reduce the stochastic switching and result into more stable molecular junction. Moreover, the weak amine coupling to the electrode implies the decreased junction "transparency" for electron current. What is the reason for well-defined, stable conductance

of amine anchored single-molecular junctions? Why do amine terminated molecules tend to form single molecular junctions? These are the questions which interest us here.

Our paper is organized as follows. In section II, we present computational and theoretical methods. In section III, we address three important aspects of the interface chemistry and their roles in the electron transport: (i) possible adsorption sites for amines and thiolates on clean and undercoordinated Au(111) surfaces, (ii) sensitivity of electron transport to the interface geometry, (iii) conductance evolution as the junction is formed and stretched by the STM tip. In section III, we also analyze and discuss these results and elucidate the nature of the well-defined conductance of amine terminated molecular junctions. Section IV summarizes the main results of our study.

II. COMPUTATIONAL METHODS

We used three computer programs in our calculations: SIESTA code⁷ to study adsorption of molecules on Au surface, ATK package^{8,9} to compute transmission spectra for all possible adsorption geometries, and our own code for "on-the-fly" conductance calculations to model STM break junction experiments. In all our calculations we use the same level of electronic structure theory. Namely, we apply density functional theory (DFT) with general gradient approximation (GGA-PBE) for the exchange-correlation potential.¹⁰ We use numerical single- ζ with polarization (SZP) for Au and the rest of the atoms are described by numerical double- ζ with polarization (DZP) basis sets.⁷ The core electrons are modeled with the Troullier-Martins nonlocal pseudopotentials.¹¹

A. Conductance calculations for static junctions

ATK program is based on the combination of the non-equilibrium Green's functions (NEGF) and DFT.^{8,9} We describe below the details of the ATK program relevant to our applications. The program uses the surface DFT calculations to obtain the electrode self-energy.⁸ The matrix product of the Green's function and the imaginary part of the left/right electrode self-energy is used to define the spectral density. The non-equilibrium, voltage-dependent density matrix is computed from the spectral density. Then the density matrix is converted into non-equilibrium electron density. The non-equilibrium electron density yields the Green's function for the scattering region. The Hartree potential is determined by the solution of the Poisson equation with voltage-dependent boundary conditions. This iterative step [Green's function \rightarrow nonequilibrium electron density \rightarrow Green's function] is repeated until the self-consistency is achieved. Then, the transmission spectrum is calculated by the standard equation.⁸

B. Junction formation and stretching: on-the-fly conductance calculations

We would like to model the experiments where the molecular junctions are formed by repeatedly crashing an Au STM tip into and pulling it out of Au surface in a molecular solution.^{2,3,4,5,6} To model these experimental conditions we developed the computational method which calculates molecular conductance "on-the-fly". Namely, we performed conductance calculations along the trajectory, which is computationally obtained by pulling the molecule from the Au electrode.

The geometry evolutions of the molecular junctions are obtained by constrained geometry relaxation method.¹² The molecular junction is aligned along the z-axis. The z coordinate of the top C atom is incremented by 0.05 Å on every step and this stretch of the junction is followed by the constrained geometry relaxation. In the constrained geometry relaxation, the z coordinate of the central bottom Au atom of the electrode cluster and the top C atom of the phenylamine or phenylthiolate molecule are fixed and the rest of the system is fully optimized. The upper electrode is the mirror image of the bottom one. The junction evolution is represented by the trajectory composed of the optimized geometries. It becomes the true molecular dynamics trajectory in the limit of extremely slow pulling speed. Previous studies found that the constrained geometry relaxation method gives the results consistent with Car-Parrinello molecular dynamics simulation of pulling molecules from surface.^{12,13}

For every step along the trajectory the conductance is computed by the method, which we implemented in the SIESTA program.⁷ We compute the self energy by the level broadening model, which has been successfully applied to molecular junctions and metal

nanowires.^{14,15} In this model, electrode energy levels are broadened to obtain the density of states, which is related to the imaginary part of self energy. Our transport implementation avoids the computationally expensive Cauchy principal value numerical integration and uses the Lorentz broadening instead, as was suggested in our non-orthogonal Wannier-type atomic orbital electron transport calculations.¹⁵ The Lorentzian broadening σ in the electrode density of state is equivalent to positive infinitesimal σ in the electrode Green's function:¹⁵

$$\mathbf{g} = [(E + i\sigma)\mathbf{S} - \mathbf{H}]^{-1}, \quad (1)$$

where \mathbf{S} is the overlap matrix and \mathbf{H} is the electrode Hamiltonian. The conductance of monoatomic gold chain attached to two gold clusters is $G_0 = 2e^2/h$,¹⁶ and the broadening parameter σ is fitted to reproduce this value. This fitting leads to $\sigma=0.5$ eV and we use this value in all our calculations. This computational method enables us to perform conductance calculations for hundreds of sample geometries from a junction evolution trajectory.

III. RESULTS AND DISCUSSION

A. Phenylamine and phenylthiolate adsorption on clean and undercoordinated gold surfaces

First principles studies of adsorption of different amine or thiolate terminated molecules on Au(111) surfaces have been reported.^{17,18,19,20} It was predicted that ammonia is adsorbed on the atop site.¹⁷ The cluster model calculations show that the adsorption energy depends significantly on the employed theoretical method.¹⁸ Phenylthiolate is attached to the bridge site and the phenyl ring is strongly tilted with respect to the Au surface.²⁰ Although previous studies are very informative, a comparative study of adsorption of amines and thioliates on Au surfaces in the context of electron transport calculations is necessary.

We represent Au(111) surface by unit cell, which is periodically repeated in two directions. The unit cell consists of five (4×4) layers of Au atoms. The undercoordinated gold surface is modeled by adding an extra apex atom above the Au(111) hollow site.

We perform geometry optimizations for phenylamine and phenylthiolate molecules adsorbed on clean and undercoordinated Au(111) surfaces. A final optimized structure is sensitive to initial guess for geometry optimization. We choose various starting geometries to explore all possible adsorption sites. Fig.1 shows atop, bridge and hollow sites on Au(111) surface. There are two different hollow sites on Au(111) surface: fcc-hollow and hcp-hollow sites. We initially align the phenyl ring of the phenylamine and phenylthiolate along the Au-Au or the Au-hollow directions. The phenyl ring of phenylamine and phenylthiolate can be perpendicular or tilted with respect to the Au surface. For tilted phenylamine,

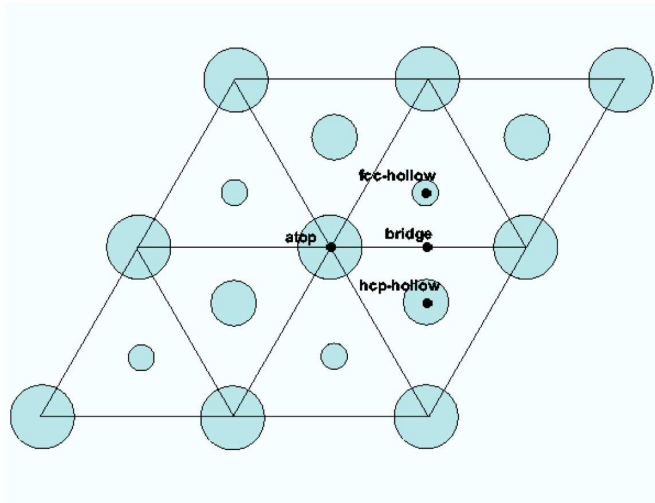


FIG. 1: Diagram which shows possible adsorption sites on Au(111) surface. The Au atoms are represented by circles of different sizes. The smaller the spheres, the farther from the layer the Au atoms are.

TABLE I: Adsorption geometries of phenylamine and phenylthiolate. N_{Au} is the number of the nearest neighbor Au atoms for the N atom or the S atom. $d_{\text{Au-N}}$ and $d_{\text{Au-S}}$ are the mean distances for the N_{Au} nearest neighbors of the N atom and the S atom respectively. θ is the angle between the phenyl ring and the surface (Fig.1 a).

phenylamine				
adsorption geometry	N_{Au}	$d_{\text{Au-N}}(\text{\AA})$	$\theta(\text{degree})$	AE (eV)
Fig.2 (b)	1	2.90	0.83	1.92
Fig.2 (c)	2	3.05	87.5	0.68
Fig.2 (d)	1	2.34	87.9	1.18
Fig.2 (e)	1	2.30	12.0	0.92
phenylthiolate				
adsorption geometry	N_{Au}	$d_{\text{Au-S}}(\text{\AA})$	$\theta(\text{degree})$	AE (eV)
Fig.2 (f)	2	2.56	8.12	3.64
Fig.2 (g)	3	2.44	89.2	2.57
Fig.2 (h)	3	2.51	63.7	2.72
Fig.2 (i)	1	2.31	31.5	2.72
Fig.2 (j)	1	2.31	51.3	2.75

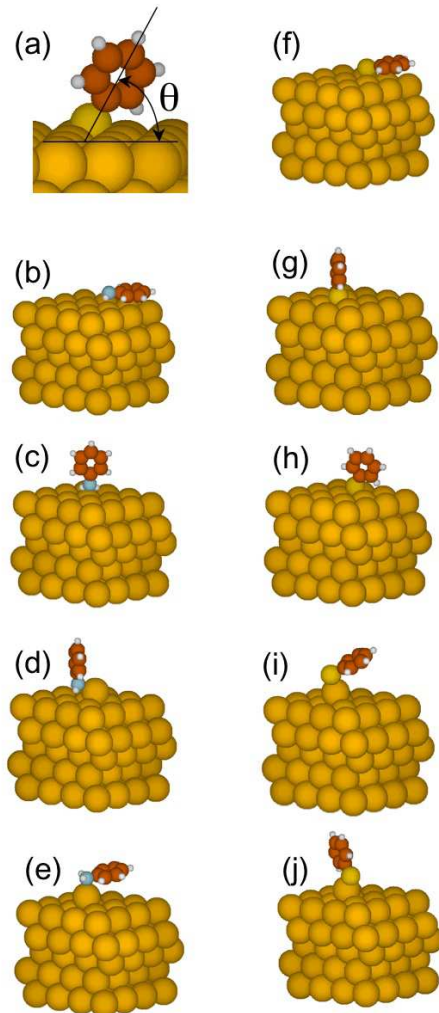


FIG. 2: adsorption geometries for phenylamine (b-e) and phenylthiolate (f-j) on the clean (b,c,f,g,h) and undercoordinated (d,e,i,j) Au(111) surfaces. (a) defines the angle θ , which is used in Table I.

the initial orientation is chosen in such a way that the N lone pair points perpendicular to the surface. We choose angle 30° for the initial phenylthiolate tilted orientation. The coordinates of the Au atoms in the two bottom layers are constrained to theoretical bulk geometry with lattice vector 4.132 \AA . This lattice vector is

obtained by performing a series of bulk calculations with different lattice parameters and fitting the energies to the third-order Birch-Murnaghan equation of state.²¹ We performed two subsequent geometry optimizations to get equilibrium structures for the adsorbed molecules. In the first geometry optimization, the N atom or the S atom (and the Au apex atom when the surface is undercoordinated) are fixed on a specific adsorption site and can only move in the z direction, which is perpendicular to the surface. In the second one, all atoms except the two bottom Au layers are fully relaxed.

Having obtained the optimized geometries for the molecules adsorbed on the surface, we compute adsorption energy (AE) by subtracting the energy of the total system from the sum of energies of the surface and the molecule.²² Fig.2 and Table I summarize the results of the geometry optimizations. Due to the failure of DFT GGA exchange-correlation functionals to account for van der Waals interactions, the actual AEs may be somewhat higher than the calculated values. AE is mainly determined by the orientation of the phenyl ring with respect to the surface. When the phenylamine is adsorbed on the clean Au (111) surface its phenyl ring either lies almost flat on the surface (geometry (b) on Fig. 2) or stays vertical to the surface (geometry (c) on Fig. 2). AE of geometry (b) is about 1.2 eV larger than that of geometry (c). This can be expected since there is strong attractive interaction between the molecular π -electrons and the metal surface image charges, which favors parallel to the surface phenyl ring orientation. The phenyl ring lies above the three-Au triangle on the Au(111) surface. The differences in the adsorption positions of the N atom cause only small AE variations of about 0.1 eV, if the phenylamine is attached vertically to the surface. When the phenylamine is adsorbed on undercoordinated Au(111) surface, the phenylamine adopts vertical (geometry (d) on Fig. 2) or tilted (geometry (e) on Fig. 2) configurations. The N lone-pair points to the apex Au atom in both cases. AE of the vertical phenylamine (1.18 eV) is 0.26 eV larger than that of the tilted one, and it is 0.50 eV larger than AE of the most stable non-lying adsorption geometry on clean Au(111) surface.

The geometry optimizations of phenylthiolate on clean Au(111) surface also yield adsorption structures where the molecule either lies almost flat on the surface (f), or it is vertical (g), or it is tilted (h) with respect to the surface. The lying phenylthiolate is not perfectly parallel to the surface, because the attraction between the S atom and the surface pulls the atom closer to the surface. In agreement with previous calculations,²⁰ the S atom appears near the bridge site in the lying geometry. If phenylthiolate is adsorbed on the apex Au atom, the molecule is always tilted with respect to the surface. For phenylthiolate, there are two possible tilted geometries. The phenyl ring plane is tilted in the first geometry ((i) on Fig. 2), and the second geometry has the vertical phenyl ring but the tilted S-C-C axis ((j) on Fig. 2). The AE difference of these two possible tilted geometries

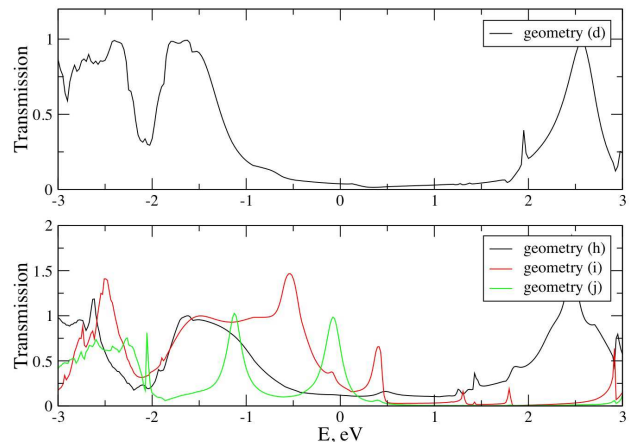


FIG. 3: Transmission spectra of BDA (upper panel) and BDT (lower panel) computed for different adsorption geometries. Fermi energy of the electrodes is shifted to zero. The junction geometries (d), (h),(i) and (j) refer to Table I and Fig.2.

is within 0.1 eV. The lying adsorbed molecule also gives the largest AE for phenylthiolate. But unlike phenylamine, the tilted adsorption geometries of phenylthiolate on clean and undercoordinated Au(111) surface have very similar AEs, which are about 0.9 eV smaller than that for the lying geometry and 0.15 eV larger than AE for the vertical geometry.

B. Electron transmission dependence on adsorption site geometry

Fig.2 and Table I list the most probable geometries for the adsorption of phenylamine and phenylthiolate on Au(111) surface. These configurations are obtained from the geometry optimizations described in the previous section. The lying on the surface molecular junctions (Fig.2 (b), (e), (f)) are excluded from the transport calculations, since it is difficult to form them experimentally. Our calculations show that their conductance is close to or even larger than the conductance of a gold monoatomic wire, $G_0 = 2e^2/h$. It means that the lying on the surface junctions are also undetectable in the STM break-junction experiments. Three different geometrical arrangements (h), (i), (j) are energetically and sterically possible for BDT junction to the Au surface, whereas only one geometry (d) is available for the BDA junction. Given these optimized adsorption geometries, the molecular junctions are constructed by mirror addition of the other electrode and the corresponding anchoring group. The conductances of these four junctions are calculated by NEGF/DFT as is implemented in the ATK package.^{8,9} Transmission spectra of the BDA and the BDT junctions are plotted in Fig.

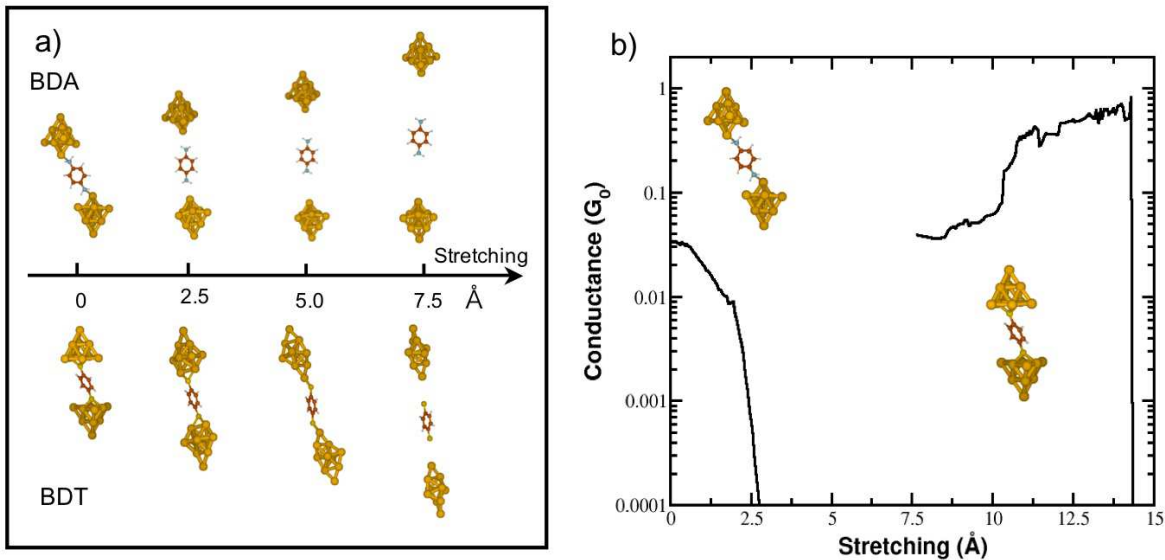


FIG. 4: a) Snapshots of the junction geometries. b) Conductance traces of the BDA (left curve) and the BDT (right curve) junctions. The starting point of conductance traces for the BDT junctions is shifted along the x axis to 7.5 Å. Inset: the starting junction geometries.

3. The BDA transmission is featureless in the vicinity of the Fermi energy. Fig.3 shows very distinct transmission spectra for three geometrically different BDT junctions which have similar AEs. The BDT junction with geometry (h) does not have any transmission resonances near the electrode Fermi energy. The junction with geometry (i) shows two resonances: one broad resonance is below and one resonance is above the Fermi energy. The most "transparent" for electrons junction is the junction with geometry (j). It has one peak located at the Fermi energy. The transmission spectra for the BDT junctions are in quantitative agreement with the results of density functional theory based electron transport calculations reported by other authors.^{23,24,25}

The Landauer formula²⁶

$$G = G_0 T(E_F) \quad (2)$$

relates the conductance G with the transmission func-

tion $T(E_F)$ computed at the Fermi energy E_F of the electrodes. This linear relation is valid when the applied voltage bias is small.²⁶ It is sufficient for our applications since very low voltage (10-25 mV) is used in STM break junction experiments.^{2,5}. Therefore the conductance for BDA and BDT junctions can be extracted from the transmission spectra plotted on Fig. 3. The conductance of the BDA junction is $0.038 G_0$. The experimentally measured conductance for BDA junction is $0.0064 G_0$ (reported in Ref.⁵) that is 6 times smaller than the computed value. The reason for this discrepancy is not clear. The BDT junction shows a wide range of conductance values: $0.1 G_0$ for geometry (h), $0.2 G_0$ for geometry (i), and $0.7 G_0$ for geometry (j). Such variations are qualitatively consistent with the experimental observation that the mean conductance variation for amine anchored junction is much smaller than that for thiolate linked junction in different experimental conductance traces.⁵

Our study demonstrates that BDA adsorbs on apex Au atom, while BDT can be adsorbed on both clean Au surface and apex Au atom. It means that there are more geometrical constraints for BDA than for BDT in forming junctions. In addition, the N lone-pair leads to the stronger orientation preference for the amine-Au bond than that for the thiolate-Au linkage. Therefore, it is sterically more difficult to get multiple BDA molecules in a junction. Based on this picture, we suggest that the recently studied dithiocarbamate and dithiocarboxylate anchoring groups,^{27,28,29} which are even more constrained orientationally, would provide stable and well-defined junctions for experimental measurements.

C. Conductance Trace Calculations

We model STM break-junction experiments by our program for "on-the-fly" conductance calculations. We use the most stable non-lying adsorption geometries of phenylamine and phenylthiolate ((d) and (j) respectively on Fig.2) to prepare the cluster models for the conductance trace calculations. The atomic coordinates of the 10-atom gold cluster and the molecule are extracted from the optimized adsorption geometry. Then we perform 150 constrained geometry relaxations for each cluster-molecule system as is described in section II B. This series of the constrained geometry relaxations yields the trajectories which describe the evolution of the junction when the molecule is pulled from the Au surface by the STM tip. Each trajectory uniformly spans the junction evolution from the equilibrium stretch 0 \AA to $150 \times 0.05 \text{ \AA} = 7.5 \text{ \AA}$. Fig.4(a) shows representative snapshots of the geometry evolutions for the BDA and BDT junctions.

The junctions undergo completely different geometry evolutions as they are stretched. The pulling of BDT causes the significant distortion of the Au cluster, which represents the electrode. At the same time, the geometry of the Au cluster is not significantly affected by the stretching of the BDA junction. This can be understood by comparing amine-Au and thiolate-Au bond strengths. The amine-Au is a weak bond. When BDA is pulled from the Au electrode, the bond between the amine and the apex Au atom ruptures before the molecule is able to involve the other Au atoms from the cluster into its motion. The interaction between thiolate and Au is considerably stronger than Au-Au interaction, and it involves all Au atoms into the motion as the BDT junction is stretched. Therefore, the electrode geometry evolution for the BDA junction is characterized by two states (before and after the amine-Au bond rupture), whereas the BDT junction has different electrode geometries for every stretching step.

Junction conductance traces and the geometry evolution trajectories are calculated simultaneously (see section II B for detail). Fig. 4 shows the conductance traces for the both junctions. The conductance of BDA only slightly fluctuates around several hundredth of G_0

at early stage of the pulling, then it drops abruptly when the amine-Au linkage ruptures. Oppositely, the BDT junction undergoes almost two orders of magnitude variation in the conductance before the molecule is detached from the electrode. This difference of the behavior of the conductance variations is consistent with the experimental observations.⁵ We also noticed that the conductance of the BDT junction is increased as the junction is stretched by the STM tip. This behavior of the the conductance trace is in agreement with Xue and Ratner observation that the the conductance of BDT may grow with the increase in the molecule-electrode separation.²³ It is also consistent with Ke, Baranger and Yang calculations which show that the presence of an additional Au atom at each of the two contacts will increase the BDT conductance.²⁵

IV. CONCLUSION

We performed a computational study to elucidate the nature of the well-defined conductance of amine terminated molecular junctions. We analyzed possible adsorption geometries of amines and thioliates on clean and undercoordinated Au(111) surfaces. Electron transport properties of BDT and BDA molecules are computed for static junctions as well as "on-the-fly" to model STM break junction experiments. The main results of our study can be summarized as follows:

1. Amines adsorb only on undercoordinated Au surface whereas thioliates adsorb equally well on clean and undercoordinated Au surfaces. AE of the vertical phenylamine on undercoordinated Au(111) surface is 0.50 eV larger than AE of the most stable non-lying adsorption geometry on clean Au(111) surface. AEs of phenylthiolate on on clean and undercoordinated Au(111) surface are very similar ($\sim 2.7 \text{ eV}$).
2. The number of accessible geometries for BDA junction on Au surface is much smaller than that for the BDT. Only one geometry is sterically/energetically accessible for BDA junctions whereas three different geometries are possible for BDT. It suggests it is more likely for the amine terminated molecules to form single molecule junctions than for thiolate terminated molecules.
3. Conductance of static BDA junction is $0.0064 G_0$ whereas conductance of BDT varies from 0.1 to $0.7 G_0$ depending on the adsorption geometry.
4. The conductance of BDA only slightly fluctuates at the early stage of the junction formation, then it drops abruptly as the amine-Au linkage ruptures. Oppositely, the BDT junction undergoes almost two order of magnitude variation in the conductance before the molecule is detached from the

electrode. This is because the electrode geometry is significantly distorted by the thiolate anchored junction stretch and is not affected by the stretch of the amine anchored junction.

Acknowledgment. The authors are grateful to M. Gelin for helpful discussion. This work was partially supported by the American Chemical Society Petroleum Research Fund (44481-G6).

-
- ¹ Nitzan, A.; Ratner, M. A. *Science*, **2003**, 300, 1384.
² Xu, B.Q.; Tao, N.J. *Science*, **2003**, 301, 1221.
³ Tao, N.J. *J. Material Chem.*, **2005**, 5, 3260.
⁴ Xiao, X.; Xu, B.; Tao, N. *J. Nano Lett.* **2004**, 4, 267.
⁵ Venkataraman, L.; Klare, J. E.; Tam, I. W.; Nuckolls, C.; Hybertsen, M. S.; Steigerwald, M. L. *Nano Lett.* **2006**, 6, 458.
⁶ Venkataraman, L.; Klare, J.E.; Nuckolls, C.; Hybertsen, M. S.; Steigerwald, M. L. *Nature* **2006**, 442, 904.
⁷ Soler, J. M.; Artacho, E., Gale, J.; Garcia, A., Junquera, J.; Ordejon, P.; Sanchez-Portal, D. *J. Phys.: Condensed Matter* **2002**, 14, 2745-2779.
⁸ Brandbyge, M.; Mozos, J.-L.; Ordejon, P.; Taylor, J.; Stokbro, K. *Phys. Rev. B* **2002**, 65, 165401.
⁹ ATK version 2.0, Atomistix A/S (www.atomistix.com).
¹⁰ Perdew, J. P.; Burke, K.; Ernzerhof, M. *Phys. Rev. Lett.* **1996**, 77, 3865.
¹¹ Troullier, N; Martins, J. L. *Phys. Rev. B* **1991**, 43, 1993.
¹² Kruger, D.; Rousseau, R.; Fuchs, H.; Marx, D. *Angew. Chem. Int. Ed.* **2003**, 42, 2251.
¹³ Kruger, D.; Fuchs, H.; Rousseau, R.; Marx, D.; Parrinello, M. *Phys. Rev. Lett.* **2002**, 89, 186402.
¹⁴ Tada, T.; Kondo, M.; Yoshizawa, K. *J. Chem. Phys.* **2004**, 121, 8050.
¹⁵ Li, Z.; Kosov, D. S. *J. Phys.: Condensed Matter* **2006**, 18, 1347.
¹⁶ Agrait, N.; Yeyati, A.L.; van Ruitrbeek, J.M. *Phys.Rep.* **2003**, 377, 81.
¹⁷ Bilic, A.; Reimers, J. R.; Hush, N. S.; Hafner, J. *J. Chem. Phys.* **2002**, 116, 8981-8987.
¹⁸ Lambropoulos, N. A.; Reimers, J. R.; Hush, N. S. *J. Chem. Phys.* **2002**, 116, 10277-10286.
¹⁹ Zhou, J.-G; Hagelberg, F. *Phys. Rev. Lett.* **2006**, 97, 45505.
²⁰ Bilic, A.; Reimers, J. R.; Hush, N. S. *J. Chem. Phys.* **2002**, 122, 94708.
²¹ Birch, F. *Phys. Rev.* **1947**, 71, 809.
²² We assume that all H atoms released upon the adsorption of phenylthiols form H₂ molecules. Therefore, the chemical potential of the H atom in H₂ is added to the total energy of the adsorbed system, when AE of phenylthiolate is computed.
²³ Xue, Y.; Ratner, M.A. *Phys. Rev. B* **2003**, 68, 115407
²⁴ Evers, F.; Weigend, F.; Koentopp, M. *Phys. Rev. B*, **(2004)**, 69, 235411.
²⁵ Ke, S.H.; Baranger, H.U.; Yang, W. *J. Chem. Phys.* **2005**, 122, 074704.
²⁶ Datta, S. *Electronic Transport in Mesoscopic Systems* (Cambridge University Press, Cambridge, 1995)
²⁷ Tivanski, A. V.; He, Y.; Borguet, E.; Liu, H.; Walker, G. C.; Waldeck, D. H. *J. Phys. Chem. B* **2005**, 109, 5398.
²⁸ Li, Z.; Kosov, D. S. *J. Phys. Chem. B* **2006**, 110, 9893.
²⁹ Li, Z.; Kosov, D. S. *J. Phys. Chem. B* **2006**, 110, 19116